



ELSEVIER

Physics of the Earth and Planetary Interiors 92 (1995) 119–141

PHYSICS
OF THE EARTH
AND PLANETARY
INTERIORS

A self-consistent convection driven geodynamo model, using a mean field approximation

C.A. Jones^{a,*}, A.W. Longbottom^a, R. Hollerbach^b

^a Department of Mathematics, Exeter University, Exeter EX4 4QE, UK

^b IGPP, Los Alamos National Laboratory, Los Alamos NM 87545, USA

Received 14 February 1995; revision accepted 28 April 1995

Abstract

The magnetic fields generated by thermal convection in a rapidly rotating fluid spherical shell are studied. The shell is sandwiched between a finitely conducting solid inner core and a non-conducting mantle. As the Rayleigh number is increased, the convective motion becomes stronger; when the magnetic Reynolds number becomes larger than a few hundred, dynamo action onsets, and a magnetic field with both axisymmetric and nonaxisymmetric components develops. The magnetic fields generated are generally of the same order of magnitude as the geomagnetic field, and the outer core fluid velocity is consistent with the values deduced from secular variation observations.

A mean field approximation is used in which the dynamics of one non-axisymmetric convective mode (the $m = 2$ mode being most frequently used) and the associated axisymmetric components are followed. This scheme involves significantly less computation than a fully three-dimensional code, but does not require an arbitrary α -effect to be imposed.

Although the Roberts number, q , the ratio of thermal to magnetic diffusion, is small in the Earth, we find that dynamo action is most easily obtained at larger values of q . The Ekman number in our calculations has been taken in the range $O(10^{-3})$ – $O(10^{-4})$, which, although small, is larger than the appropriate value for the Earth's core. At $q = 10$ we find solutions at Rayleigh numbers close to critical; two such runs are presented, one corresponding to a weak field dynamo, another to a strong field dynamo; the solution found depends on the initial conditions. At $q = 1$, the solutions have a complex spatial and temporal structure, with few persistent large-scale features, and our solutions reverse more frequently than the geodynamo. The final run presented has an imposed stable region near the core–mantle boundary. This solution has a weaker non-axisymmetric field, which fits better with the observed geomagnetic field than the solution without the stable layer.

1. Introduction

A central problem in modelling the geodynamo is that the dynamo process is intrinsically

three-dimensional. Not only is there evidence of substantial departures from axisymmetry in both the magnetic field and the flow pattern in the outer core, but also Cowling's (1934) theorem tells us that the non-axisymmetric components of the field are an essential part of the dynamo

* Corresponding author.

process. Furthermore, if the dynamo is powered by convection, whether thermal or compositional, there are strong theoretical reasons indicating that the convection pattern will be non-axisymmetric. Although the first steps towards fully three-dimensional modelling of the geodynamo have been taken (Zhang and Busse, 1988, 1989, 1990; Glatzmaier and Roberts, 1995; Hirsching and Busse, 1995) computers are not yet powerful enough either to reach the right parameter range for the geodynamo or to allow exploration of the parameter space. A further difficulty is that those convective dynamos found so far which have simple time dependence (either stationary or periodic) are all weak field models, in which the magnetic field does not significantly influence the convection; known dynamos which have strong fields (Elsasser number $O(1)$) influencing the convection all have chaotic time dependence. As the magnetic field in the Earth's core almost certainly has Elsasser number $O(1)$, this adds greatly to the difficulty, as it is necessary to integrate for very long times to convince oneself that the field in the model will not ultimately decay (Hughes, 1993).

The traditional way to avoid the difficulties of fully three-dimensional computations has been to introduce an α -effect into the induction equation, which can regenerate poloidal field from toroidal field and hence allow axisymmetric models. The use of the α -effect can be justified either by assuming that the non-axisymmetric components are small (Braginsky, 1976) or by assuming that turbulent non-axisymmetric components of the flow are on a small length scale (Krause and Rädler, 1980). The resulting models have been extensively studied in the linear (kinematic) regime and also in the nonlinear regime, where they are often known as intermediate models.

A number of important issues have been investigated using intermediate models, and this previous work has implications for three-dimensional convective models. The existence (or otherwise) of Taylor (1963) states, solutions independent of viscosity, is of interest because even if the outer core is turbulent, the Ekman number is very small. α^2 models have been studied by Soward and Jones (1983) in plane layer geometry, and by

Hollerbach and Lerley (1991) and Barenghi (1992) in spherical geometry. They all found solutions which satisfied Taylor's constraint in accordance with the Malkus–Proctor (1975) scenario (see also Proctor (1977)). $\alpha\omega$ models have been studied by Abdel-Aziz and Jones (1988) in plane layer geometry, and by Jones and Wallace (1992) in a duct geometry. They too found Taylor states. Initial calculations on the model-Z (Braginsky, 1976, 1978; Braginsky and Roberts, 1987; Roberts, 1989) $\alpha\omega$ -dynamo suggested that Taylor states did not exist, but more recent work by Jault (1995) at lower Ekman number indicates that this $\alpha\omega$ model also eventually attains a Taylor state. Jault also found that dynamo models are more likely to achieve a Taylor state as the strength of the α -effect is increased if both quadrupole and dipole modes are allowed, even if the initial linear instability is purely dipolar.

Although much has been learnt from these models, a serious problem is that the distribution of the turbulence in the outer core is unknown, and it is difficult to see how it could be found in the foreseeable future. In consequence, the distribution of the α -effect in the outer core is uncertain; in practice it has to be arbitrarily imposed. This might be reasonable if it were the case that dynamo models were largely independent of the α distribution, but unfortunately there is now overwhelming evidence that the behaviour of particular models is very dependent on the form of α assumed. For example, the much studied model-Z of Braginsky has a highly specific α distribution which leads to a steady dynamo and a meridional circulation which maintains approximate steadiness into the nonlinear regime. In contrast, the simpler distributions of α chosen by Barenghi and Jones (1991), Hollerbach et al. (1992), Barenghi (1993) and Anufriev et al. (1995) led to dynamos which are oscillatory both in the linear and nonlinear regimes.

It is therefore desirable to abandon the arbitrary α -effect, and turn instead to nonaxisymmetric convection driven dynamo models. In these models, the convection process believed to drive the dynamo is included in the calculation. There is therefore much less arbitrariness about the model. There are still unknown parameters, and

uncertainties about the nature of the convection, but this approach does allow us to test specific hypotheses by comparison with geomagnetic data. Because of the difficulties inherent in a fully three-dimensional attack outlined above, we have adopted what might be described as a $2\frac{1}{2}$ -dimensional approach: in spherical polars r , θ and ϕ the radial (r) and meridional (θ) directions are fully resolved, but in the decomposition $\exp(im\phi)$ only one nonaxisymmetric wavenumber m is included along with the axisymmetric fields. We are therefore neglecting the quadratic interactions between nonaxisymmetric modes, but retaining all other nonlinear terms. This approach has been tried previously by Fearn and Proctor (1984, 1987) and in spirit by Cuong and Busse (1981); unlike Fearn and Proctor we have used a time-dependent approach rather than attempting to iterate to a steady solution. As we see below, steady solutions have not been found, which may explain why Fearn and Proctor failed to obtain converged solutions.

This $2\frac{1}{2}$ -dimensional model is sufficient to generate poloidal field as well as toroidal field and hence produce a self-consistent dynamo; that is, one in which the magnetic field used in the magnetoconvection part of the calculation is not arbitrary, but is the field generated by the dynamo part of the calculation. Our model therefore incorporates the influence of the magnetic field on the convection. This is a vital part of the dynamo process, which in previous models has often been either highly oversimplified as ‘ α -quenching’ or omitted altogether.

As yet, the work is still in a preliminary stage, and we have not yet managed to push our codes down to the parameter values relevant to the Earth. Nevertheless, the first results are very encouraging. When the behaviour of this one-mode approach is understood, and as computers become faster, we hope to be able to extend our work to include more azimuthal modes and so work towards fully three-dimensional results. There are, of course, limitations to our $2\frac{1}{2}$ -dimensional approach; in particular, it is necessary to choose the azimuthal wavenumber a priori, so that we are not permitting the system to choose the ‘preferred’ wavenumber. In a fully three-di-

mensional calculation, a different wavenumber from our imposed one might emerge. At this stage, we can only use our experience from linear magnetoconvection calculations to tell us whether our choice of wavenumber lies in the range of nonlinearly stable wavenumbers.

However, the results from this $2\frac{1}{2}$ -dimensional model will, it is hoped, give valuable information as to the most likely parameter regimes to give successful fully three-dimensional geodynamos. We have already found that certain areas of parameter space are much more amenable than others. This approach may also enable us to explore the effects of different types of convection. Although this work is restricted to a single driving component, the inclusion of both compositional and thermal convection should be straightforward. This work reports only models with a purely dipolar symmetry, but we hope to be able to extend to include modes of both parity. With the great saving in computation over fully three-dimensional models, it may also be possible to reduce the Ekman number down to low values to see how the system behaves in the low viscosity limit. Also, as has been the case with α -effect models, this approach makes it realistic to explore the consequences of new physical effects, such as core–mantle coupling. For example, Hollerbach and Jones (1993a,b, 1995) have included a freely rotating, finitely conducting inner core in an α -effect model. They have shown that the inclusion of the inner core can have a powerful effect on the dynamics of the whole core, and can greatly stabilize the generated field, a conclusion that has subsequently been verified in a far more complicated model (Glatzmaier and Roberts, 1995). It is hoped that this model will serve a similar purpose: to explore new effects that can subsequently be tested in the more complicated model.

2. The dynamo equations

As in our α -effect (Hollerbach and Jones, 1993a,b, 1995) and magnetoconvection (Longbottom et al., 1995, hereafter referred to as LJH95) studies, the inertial terms are neglected com-

pared with the Coriolis terms, so that the Rossby number $\eta/2\Omega l_0^2$ is negligibly small. In the Boussinesq approximation the governing geodynamo equations in a frame of reference rotating about the z -axis with angular velocity $\Omega = \Omega \hat{z}$ are (Fearn, 1994)

$$\hat{z} \times \mathbf{U} = -\nabla P + (\nabla \times \mathbf{B}) \times \mathbf{B} + E \nabla^2 \mathbf{U} + q \text{Ra} T r \quad (1)$$

$$\frac{\partial \mathbf{B}}{\partial t} = \nabla^2 \mathbf{B} + \nabla \times (\mathbf{U} \times \mathbf{B}) \quad (2)$$

$$\frac{\partial T}{\partial t} = q \nabla^2 T - \mathbf{U} \cdot \nabla T + s \quad (3)$$

$$\nabla \cdot \mathbf{B} = \nabla \cdot \mathbf{U} = 0 \quad (4)$$

Here \mathbf{U} , \mathbf{B} and T are the fluid flow, field and temperature, respectively. All equations are in dimensionless form, the unit of length being $l_0 (= r_o - r_i)$, where r_o and r_i are the outer core and inner core radii, respectively; in all runs reported here we take $r_i/r_o = 1/3$. The unit of time is then the Ohmic timescale l_0^2/η , and the unit of magnetic field is $(2\Omega\mu\rho_o\eta)^{1/2}$, μ being the permeability which is close to the free space value, ρ_o being the outer core density and η being the magnetic diffusivity. The temperature is non-dimensionalized so that in the absence of convection the temperature at the inner core boundary (ICB) is 0.5 and at the core–mantle boundary (CMB) is -0.5 . For uniform heating s , the conduction profile is then $T_0 = \frac{s}{8} - \frac{1}{2}r^2$. When the usual estimates for geophysical parameters are made, our unit of time is about 60 000 years, our unit of length about 2200 km, and our unit of magnetic field is about 22 gauss = 2.2 mT.

The dimensionless parameters in the equations are

$$E = \frac{\nu}{2\Omega l_0^2}, \quad q = \frac{\kappa}{\eta}, \quad \text{Ra} = \frac{g\alpha\beta l_0^2}{2\Omega\kappa}$$

the Ekman number, the Roberts number, and the modified Rayleigh number, respectively. Here η is the magnetic diffusivity, ν is the coefficient of kinematic viscosity, κ is the thermal diffusivity and $-g\mathbf{r}$ is the acceleration due to gravity (taken to act radially inwards). The coefficient of expansion is α and βl_0 is the unit of temperature.

We decompose the magnetic field, fluid flow and temperature into axisymmetric and non-axisymmetric components. In the following, the barred variables represent the unperturbed, axisymmetric parts of the physical state and the unbarred variables the corresponding non-axisymmetric perturbation. Thus the magnetic field $\mathbf{B} = \bar{\mathbf{B}} + \mathbf{b}$, the flow $\mathbf{U} = \bar{\mathbf{U}} + \mathbf{u}$, the temperature $T = T_0 + \bar{T} + T'$ and the pressure $P = \bar{P} + p$. The term T_0 in the temperature decomposition is the conduction profile.

The approximation which reduces the system from fully three-dimensional to $2\frac{1}{2}$ -dimensional is the neglect of the nonaxisymmetric parts of those terms which are quadratic in nonaxisymmetric terms. Thus, in general, there will, for example, be a nonaxisymmetric part arising from the term $(\nabla \times \mathbf{b}) \times \mathbf{b}$ in (5) below, but we ignore this. If the amplitudes of the nonaxisymmetric terms are small, this will be a good approximation. When the nonaxisymmetric terms are of the same order of magnitude as the axisymmetric terms, ignoring these higher-order interactions cannot be rigorously justified; nevertheless, we believe that useful qualitative information about dynamo action can be gained from this approximation. The non-axisymmetric equations are then the same as for the magnetoconvection problem, with the difference that the axisymmetric (barred) quantities are no longer constant, but determined by a second set of equations.

The non-axisymmetric equations are

$$\mathbf{z} \times \mathbf{u} = -\nabla p + [(\nabla \times \bar{\mathbf{B}}) \times \mathbf{b} + (\nabla \times \mathbf{b}) \times \bar{\mathbf{B}}] + E \nabla^2 \mathbf{u} + q \text{Ra} T' r \quad (5)$$

$$\frac{\partial \mathbf{b}}{\partial t} = \nabla^2 \mathbf{b} + \nabla \times [\bar{\mathbf{U}} \times \mathbf{b} + \mathbf{u} \times \bar{\mathbf{B}}] \quad (6)$$

$$\frac{\partial T'}{\partial t} = q \nabla^2 T' - \bar{\mathbf{U}} \cdot \nabla T' - \mathbf{u} \cdot \nabla (\bar{T} + T_0) \quad (7)$$

$$\nabla \cdot \mathbf{b} = \nabla \cdot \mathbf{u} = 0 \quad (8)$$

As the amplitude of the nonlinear terms in this approximation is determined by the adjustment of the axisymmetric quantities in the above equations, it seems appropriate to call this approach a mean field approximation.

The magnetic field in the solid inner core satisfies

$$\frac{\partial \mathbf{b}}{\partial t} + \Omega_i \frac{\partial \mathbf{b}}{\partial \phi} = \nabla^2 \mathbf{b} \quad (9)$$

$$\nabla \cdot \mathbf{b} = 0 \quad (10)$$

where Ω_i is the inner core rotation rate, and is to be determined as part of the solution. (For simplicity, we only allow the inner core to rotate about the same axis as the mantle.) As we are interested in long time-scales, the inertia of the inner core is neglected. Ω_i is then determined by the appropriate torque balance at the ICB,

$$\begin{aligned} & E r_i^3 \int_0^\pi \int_0^{2\pi} r \frac{\partial}{\partial r} \left(\frac{\bar{U}_\phi}{r} \right) \Big|_{r=r_i} \sin^2 \theta \, d\theta \, d\phi \\ & = -r_i^3 \int_0^\pi \int_0^{2\pi} (b_r b_\phi + \bar{B}_r \bar{B}_\phi) \Big|_{r=r_i} \sin^2 \theta \, d\theta \, d\phi \end{aligned} \quad (11)$$

as given by Hollerbach and Jones (1993a). The mantle is assumed insulating. The appropriate magnetic continuity conditions across the ICB and CMB are then implemented. Similarly, appropriate no-slip conditions on the flow are implemented at the ICB and the CMB, so $\bar{U} = \Omega_i r \sin \theta \hat{e}_\phi$ at the ICB.

The axisymmetric equations are

$$\begin{aligned} \hat{z} \times \bar{U} = & -\nabla \bar{P} + (\nabla \times \bar{B}) \times \bar{B} + \overline{(\nabla \times \mathbf{b}) \times \mathbf{b}} \\ & + E \nabla^2 \bar{U} + q \text{Ra} (\bar{T} + T_0) \mathbf{r} \end{aligned} \quad (12)$$

$$\frac{\partial \bar{B}}{\partial t} = \nabla^2 \bar{B} + \nabla \times (\bar{U} \times \bar{B}) + \nabla \times \overline{(\mathbf{u} \times \mathbf{b})} \quad (13)$$

$$\frac{\partial \bar{T}}{\partial t} = q \nabla^2 \bar{T} - \bar{U} \cdot \nabla (\bar{T} + T_0) - \overline{\mathbf{u} \cdot \nabla T'} \quad (14)$$

$$\nabla \cdot \bar{B} = \nabla \cdot \bar{U} = 0 \quad (15)$$

The axisymmetric magnetic field in the solid inner core satisfies

$$\frac{\partial \bar{B}}{\partial t} = \nabla^2 \bar{B}$$

$$\nabla \cdot \bar{B} = 0$$

Here the terms $\overline{(\nabla \times \mathbf{b}) \times \mathbf{b}}$, $\overline{(\mathbf{u} \times \mathbf{b})}$ and $\overline{\mathbf{u} \cdot \nabla T'}$ are the mean (or axisymmetric) parts of

the unbarred non-axisymmetric quantities and are defined by

$$\bar{f}(r, \theta) \equiv \frac{1}{2\pi} \int_0^{2\pi} f(r, \theta, \phi) \, d\phi \quad (16)$$

It should be noted that the term $\overline{(\mathbf{u} \times \mathbf{b})}$ is the mean e.m.f. familiar from the α -effect of turbulent dynamo theory. In axisymmetric turbulent dynamos this term is replaced by $\alpha \bar{B}$. The effect of the term $\overline{(\nabla \times \mathbf{b}) \times \mathbf{b}}$ was considered recently by Fearn et al. (1994) in the context of magnetoconvection, and found to be important in determining whether Taylor states arise.

In the above equations, T denotes temperature if thermal convection is assumed, but can be thought of as the density difference if compositional convection is driving, with the appropriate modifications to the definition of the Roberts and Rayleigh number. The case where both thermal and compositional effects are present simultaneously has not been considered so far. Most runs have been done with constant-temperature boundary conditions at the CMB and ICB, but fixed flux conditions have also been considered.

The nature of the observed field at the CMB (see, e.g. Gubbins and Bloxham (1987)) suggests that the following parity predominates:

axisymmetric variables:

A, v, \bar{T} symmetric about equator;

B, ψ antisymmetric about equator;

non-axisymmetric variables:

$u_r, u_\phi, b_\theta, T'$ symmetric about equator;

u_θ, b_r, b_ϕ antisymmetric about equator;

and it is this choice that is implemented here.

This symmetry assumption speeds up the computations considerably, but is not inherent in our mean field approximation.

3. The numerical method

We make the usual poloidal–toroidal decomposition of the axisymmetric and non-axisymmetric flow and field,

$$\bar{U} = \nabla \times [\psi \hat{e}_\phi] + v \hat{e}_\phi \quad (17)$$

$$\bar{B} = \nabla \times [A \hat{e}_\phi] + B \hat{e}_\phi \quad (18)$$

$$\mathbf{u} = \nabla \times [\mathbf{e}\hat{e}_r] + \nabla \times \nabla \times [\mathbf{f}\hat{e}_r] \quad (19)$$

$$\mathbf{b} = \nabla \times [\mathbf{g}\hat{e}_r] + \nabla \times \nabla \times [\mathbf{h}\hat{e}_r] \quad (20)$$

The variables ψ , v , A , B , g , h , e , f , appearing in these equations as well as the axisymmetric and non-axisymmetric temperatures \bar{T} and T' are expanded in the outer core as

$$A = \sum_{n=1}^{N1} \sum_{l=1}^{M1+2} A_{nl}^{(o)} T_{l-1}(x_o) P_{2n-1}^{(1)}(\cos \theta)$$

$$B = \sum_{n=1}^{N1} \sum_{l=1}^{M1+2} B_{nl}^{(o)} T_{l-1}(x_o) P_{2n}^{(1)}(\cos \theta)$$

$$\psi = \sum_{n=1}^{N2} \sum_{l=1}^{M2+4} \psi_{nl}^{(o)} T_{l-1}(x_o) P_{2n}^{(1)}(\cos \theta)$$

$$v = \sum_{n=1}^{N2} \sum_{l=1}^{M2+2} v_{nl}^{(o)} T_{l-1}(x_o) P_{2n-1}^{(1)}(\cos \theta)$$

$$\bar{T} = \sum_{n=1}^{N1} \sum_{l=1}^{M1+2} \bar{T}_{nl}^{(o)} T_{l-1}(x_o) P_{2n-2}^{(0)}(\cos \theta)$$

$$g = \sum_{n=1}^{N1} \sum_{l=1}^{M1+2} g_{nl}^{(o)} T_{l-1}(x_o) P_{2n+m-2}^{(m)}(\cos \theta) e^{im\phi}$$

$$h = \sum_{n=1}^{N1} \sum_{l=1}^{M1+2} h_{nl}^{(o)} T_{l-1}(x_o) P_{2n+m-1}^{(m)}(\cos \theta) e^{im\phi}$$

$$e = \sum_{n=1}^{N2} \sum_{l=1}^{M2+2} e_{nl} T_{l-1}(x_o) P_{2n+m-1}^{(m)}(\cos \theta) e^{im\phi}$$

$$f = \sum_{n=1}^{N2} \sum_{l=1}^{M2+4} f_{nl} T_{l-1}(x_o) P_{2n+m-2}^{(m)}(\cos \theta) e^{im\phi}$$

$$T' = \sum_{n=1}^{N1} \sum_{l=1}^{M1+2} T'_{nl} T_{l-1}(x_o) P_{2n+m-2}^{(m)}(\cos \theta) e^{im\phi}$$

where $P_n^{(0)}(\cos \theta)$ and $P_n^{(m)}(\cos \theta)$ are Legendre functions and associated Legendre functions, respectively, T_l are Chebyshev polynomials, with x_o being the radial coordinate normalized to $(-1, 1)$ across the spherical shell. It should be noted that the coefficients for the nonaxisymmetric quantities are all complex, the physical variable being the real part of that quantity.

In addition, as we are including a finitely con-

ducting inner core, we must expand A , B , g and h in the inner core as

$$A = \sum_{n=1}^{N1} \sum_{l=1}^{M1/2+1} A_{nl}^{(i)} T_{2l-1}(x_i) P_{2n-1}^{(1)}$$

$$B = \sum_{n=1}^{N1} \sum_{l=1}^{M1/2+1} B_{nl}^{(i)} x_i T_{2l-1}(x_i) P_{2n}^{(1)}$$

$$g = \sum_{n=1}^{N1} \sum_{l=1}^{M1/2+1} g_{nl}^{(i)} x_i^{k_1} T_{2l-1}(x_i) P_{2n+m-2}^{(m)} e^{im\phi}$$

$$h = \sum_{n=1}^{N1} \sum_{l=1}^{M1/2+1} h_{nl}^{(i)} x_i^{k_2} T_{2l-1}(x_i) P_{2n+m-1}^{(m)} e^{im\phi}$$

where $x_i = r/r_i$, and $k_1 = 2$, $k_2 = 1$ for even m , $k_1 = 1$, $k_2 = 2$ for odd m ensure the proper symmetry in r .

The numerical method used combines the techniques developed for the magnetoconvection problem (LJH95) and for the α -effect mean-field dynamo problem (Hollerbach and Jones, 1993a). The axisymmetric and non-axisymmetric equations are timestepped until initial transients have died away (taking typically 0.2 diffusion times, although it may take longer than this for initial fields to decay in regimes where dynamo action is not found) and the form of the dynamo solution becomes evident. The induction and temperature equations (6) and (7), and (13) and (14) are timestepped forward to give \mathbf{b} , T' , $\bar{\mathbf{B}}$ and \bar{T} . At each timestep the momentum equations (5) and (12) are solved to give \mathbf{u} , $\bar{\mathbf{U}}$ and Ω_i . The reader is referred to the above two references, as well as to Hollerbach (1994a,b) for further details.

The question of what initial conditions the model is started with is important; as we see below, this can affect the solution found. In this nonlinear problem there may be (and indeed apparently are) different solutions even at identical parameter values. A non-axisymmetric solution from the linear magnetoconvection problem (LJH95), together with some imposed axisymmetric field and flow, was used as the initial values for the problem. However, once a dynamo solu-

tion had been determined this was then used as the starting values for further runs.

4. Results of initial runs

Most runs have been done using 18 Chebyshev modes in the radial direction for the magnetic fields, and 18 Legendre functions for the θ dependence. The flow has a slightly higher resolution of 24 by 36. Some runs have been done with the higher resolution 24 by 24 for the field and 36 by 60 for the flow as a check on the accuracy of the solution. Our usual resolution is adequate to get down to $E \approx 5 \times 10^{-4}$. Lower values of E will require more modes and hence more computer power. The reason for taking more modes for the flow than for the field was concern over resolving the Ekman layers that occur near the boundaries of the outer core when the Ekman number is small. There is also a possibility of Stewartson layers forming at the tangent cylinder to the inner core (Hollerbach, 1994a,b). As the character of the solutions found is dependent on the parameter regime, there is unlikely to be a single best choice for distributing the modes between the field and the flow, but as the magnetic Reynolds numbers we find are generally only of the order of a few hundred, the choice of having slightly more resolution for the flow than for the field appears reasonable.

Four runs are presented here. It became apparent that the behaviour is much more unstable at lower values of q , the Roberts number, so we have concentrated on values between one and ten for this parameter. The azimuthal wavenumber has to be chosen as a parameter: in all runs we have chosen $m = 2$, which fits the observational data best (e.g. Bloxham et al., 1989), and has support from magnetoconvection theory.

In the first three runs, the uniform heating profile $5/8 - r^2/2$ has been used, which is unstably stratified throughout the outer core. This has a heat flux of $0.5 \times 4\pi r_i^2$ units entering the outer core at the ICB, and $1.5 \times 4\pi r_o^2$ leaving at the CMB, the difference being assumed to be generated internally in the outer core. Constant temperature boundary conditions have been taken at the ICB and CMB.

4.1. Run (A)

Here the Roberts number $q = 10$, the Ekman number $E = 10^{-3}$, and the Rayleigh number $Ra = 85$. The solution was started with no meridional field threading the inner core, but with the imposed toroidal field $8(r - r_i)^2[1 - (r - r_i)^2] \sin \theta \cos \theta$ which was used by LJH95 and others; this toroidal field is zero at the ICB and CMB. The nonaxisymmetric quantities were given the initial form of the linear solutions found in LJH95, but with a small amplitude. Initially, the nonaxisymmetric terms grow, but after transients have died away the axisymmetric field becomes nearly periodic with a period just over 1000 years (see Run (A), Figs. 1(a) and 1(b), and recall that

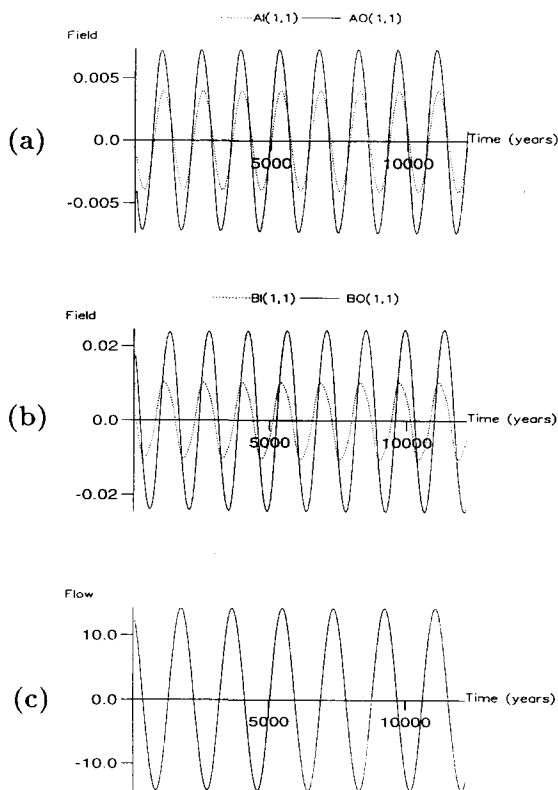


Fig. 1. The time dependence of $AI(1, 1) = A_{11}^{(i)}$, $AO(1, 1) = A_{11}^{(o)}$, $BI(1, 1) = B_{11}^{(i)}$, $BO(1, 1) = B_{11}^{(o)}$ and $E(1, 1) = e_{11}$, the leading coefficients in the expansions for the inner and outer core axisymmetric poloidal field potential, the inner and outer core axisymmetric toroidal field, and the toroidal nonaxisymmetric velocity, respectively.

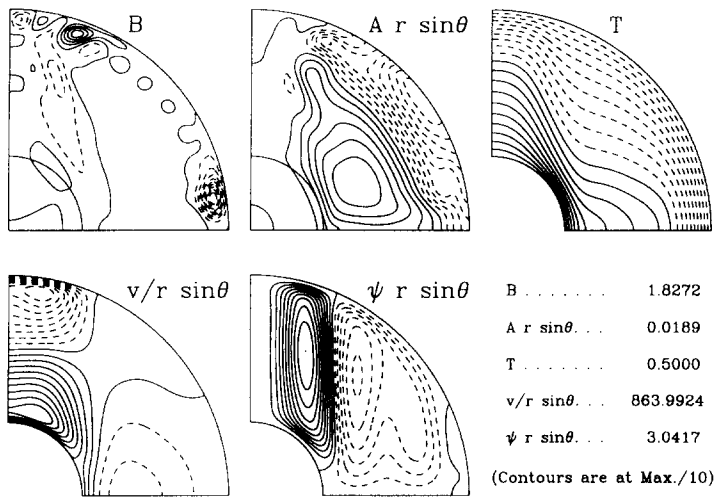


Fig. 2. Axisymmetric variables in Run (A). B , Toroidal field contours; $A r \sin \theta$, meridional field lines; T , temperature contours; $v/r \sin \theta$, angular velocity contours; $\psi r \sin \theta$, meridional stream lines. Negative contours are dashed.

the magnetic diffusion time is 60 000 years). The nonaxisymmetric field is also nearly periodic and approximately sinusoidal, but with a different frequency. In Fig. 1(c) we show one component of the convective flow variables (it makes no difference which) as a function of time to see this second frequency.

Figs. 2 and 3 show the axisymmetric and non-axisymmetric magnetic fields at one instant in the oscillation (space does not permit us to show the whole time-sequence). For the nonaxisymmetric

quantities we show real and imaginary parts, giving the form of the solution in two meridional planes 90° apart.

This solution corresponds to a weak field dynamo. The axisymmetric temperature, azimuthal velocity and streamfunction vary very little over the cycle, taking the values they would have for convection in the presence of no magnetic field. The axisymmetric poloidal field is rather weak; the nonaxisymmetric radial field at the CMB is reasonable, but as the axisymmetric dipole is too

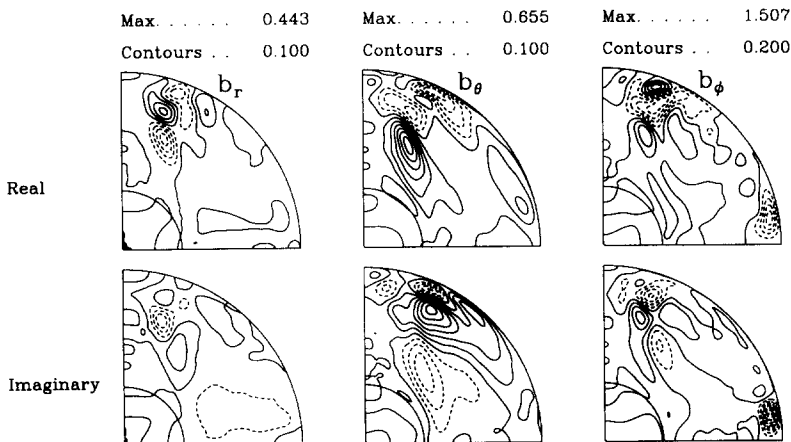


Fig. 3. Nonaxisymmetric magnetic field in Run (A). Negative contours are dashed. The maximum absolute value of each quantity is shown, together with the interval between each contour level.

weak, the field is not like the Earth's magnetic field (see Fig. 4). On this figure (and others subsequently) a cylindrically equidistant projection is used and the continents are drawn to make it possible to compare with Bloxham et al. (1989) and Bloxham and Jackson (1991). The

convection is strong, however, corresponding to magnetic Reynolds numbers going up to nearly 600 (see Fig. 5). The value of the Ekman number is not quite small enough to make convection with no magnetic field very inefficient, but it is small enough for rotation to have a strong effect

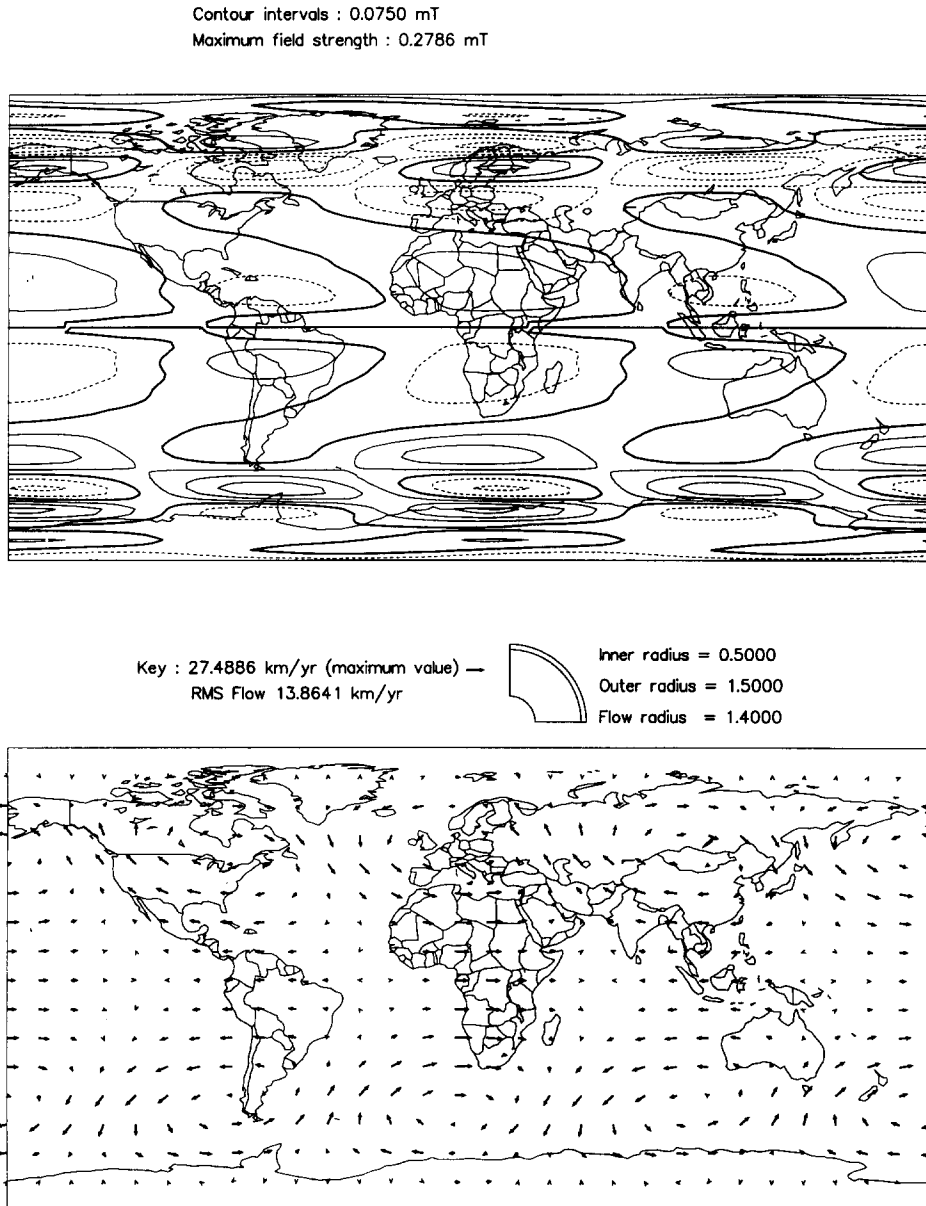


Fig. 4. Run (A). Upper part: the radial component of magnetic field at the CMB. Negative contours are dashed. Lower part: the fluid flow at a radius of 1.4 in dimensionless units.

on the dynamics. The toroidal field has a curious structure in these solutions; there are maxima near the poles and the equator, but very little field in the middle of the outer core, where the convection is strongest. Possibly this is due to flux expulsion, which would be consistent with the rather high magnetic Reynolds number. The maximum toroidal field strength is about 35 gauss.

As the non-axisymmetric quantities are governed by linear equations (5)–(8), if the axisymmetric coefficients were constant the nonaxisymmetric quantities would be proportional to $\exp[im(\phi - \omega t)]$ for some eigenvalue ω . Because of the weak field nature of this solution, this is in fact almost the case; although the magnetic field varies a lot, as the field is weak the terms involving $\bar{\mathbf{B}}$ in (5) and (6) are almost negligible, and $\bar{\mathbf{U}}$ and $\bar{\mathbf{T}}$ are almost constant in time. If the non-axisymmetric fields are $\propto \exp[im(\phi - \omega t)]$, because of the mean field approximation the nonaxisymmetric interaction terms in (9)–(11) will be almost constant in time; the frequency ω will therefore not show up in the axisymmetric variables. Of course, the magnetic field will have some small impact on the dynamics, and so the

axisymmetric coefficients of the nonaxisymmetric equations cannot be exactly constant. The solutions shown in Figs. 1(a) and 1(b) cannot therefore be exactly periodic, although the departures from periodicity are evidently very small. In this case, the convection is effectively drifting around the sphere at constant speed, providing a constant e.m.f. which drives a dynamo oscillating at an unrelated frequency.

These weak field solutions also suffer from another objection: although $m = 2$ is imposed, at low E it will not be the preferred wavenumber. Higher m will be preferred. If the Rayleigh number is reduced below about 70, the field decays exponentially, and steady drifting nonmagnetic convection rolls are left.

4.2. Run (B)

Rather remarkably, if a dipole field of reasonable strength penetrating the inner and outer core is imposed at time $t = 0$, the field does not decay even at Ra as low as 50. Indeed, a rather strong toroidal field develops which significantly alters the convection pattern. The initial condi-

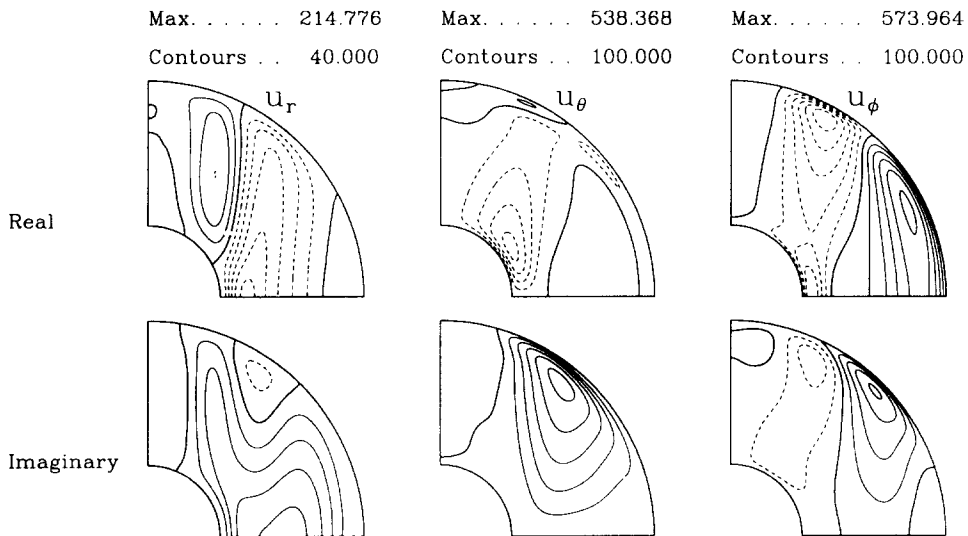


Fig. 5. Nonaxisymmetric velocity field in Run (A). Negative contours are dashed. The maximum absolute value of each quantity is shown, together with the interval between each contour level. As the dimensionless unit of velocity is based on the magnetic diffusion timescale, the contours give local magnetic Reynolds number.

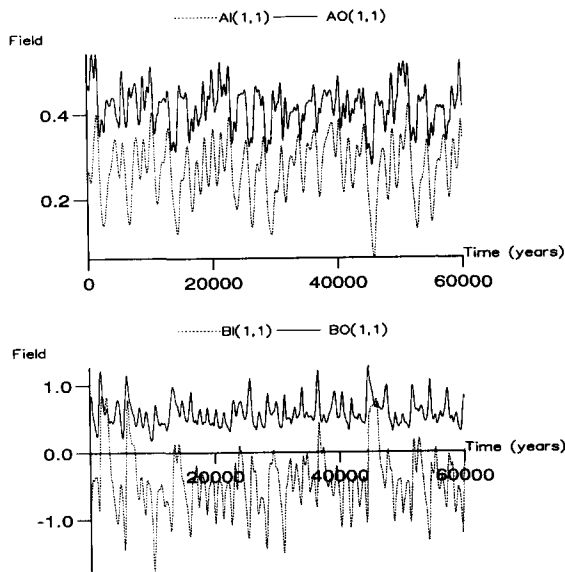


Fig. 6. The time dependence of $AI(1, 1) = A_{11}^{(i)}$, $AO(1, 1) = A_{11}^{(o)}$, $BI(1, 1) = B_{11}^{(i)}$, $BO(1, 1) = B_{11}^{(o)}$ for Run (B).

tion was the same as for Run (A), but with the important addition of an axisymmetric dipole term ($A_{11}^{(o)} = A_{11}^{(i)} = 0.2$, all other A coefficients zero).

Run (B) had $q = 10$, $E = 10^{-3}$, and $Ra = 50$.

The time dependence is somewhat chaotic (see Run (B), Fig. 6), but both the spatial and temporal dependence is well resolved at the truncation and time step (2.5×10^{-5}) used, as was checked by running with different truncations and time steps. The solution was run for a full diffusion time (60 000 years) but the meridional field did not reverse. Considerations of space make it impossible to show all the fields at all times, but to see the nature of the fields contour plots at the end of the run are shown. The toroidal field is now rather strong (maximum 130 gauss) (see Fig. 7), and although the peaks are still near the equator (and to a lesser extent the pole) there is now significant field in the convecting interior. The meridional circulation and the azimuthal flow now vary significantly with time. It should be noted that there are comparatively small regions near the axis where the angular velocity $v/r \sin \theta$ is large, driven by Lorentz forces produced mainly by the nonaxisymmetric field components.

The axisymmetric dipole component of this solution is about twice the size of the Earth's, but this is not so serious, as it may well reduce slightly with E . More serious is perhaps the large value of the non-axisymmetric field components

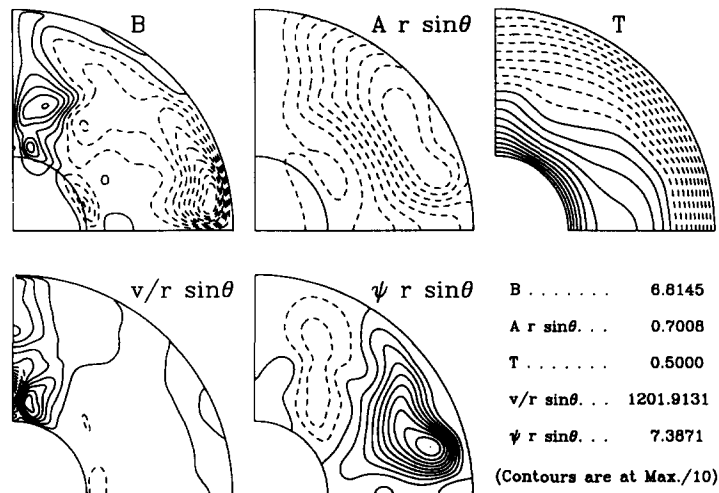


Fig. 7. Axisymmetric variables in Run (B). B , Toroidal field contours; $A r \sin \theta$, meridional field lines; T , temperature contours; $v/r \sin \theta$, angular velocity contours; $\psi r \sin \theta$, meridional stream lines. Negative contours are dashed.

(Fig. 8), even for the radial component at the CMB. This is about ten times too big (Fig. 9). It should also be noted that although the toroidal axisymmetric field is considerably stronger than the poloidal axisymmetric field, the ϕ -component of the nonaxisymmetric field is not very different in strength from the other components (Fig. 8).

The convective flow is slightly less than for the weak field solution (maximum magnetic Reynolds number 350; see Fig. 10) but the action of this flow on the large toroidal field is to produce too large a nonaxisymmetric magnetic field near the CMB. This problem was noted in our linear magnetoconvection paper L_{JH}95. A possible way out is to have the main toroidal field more concentrated near the ICB, possibly as a consequence of a stably stratified layer near the CMB.

4.3. Run (C)

The Roberts number q was reduced to unity. E is still 10^{-3} , but the Rayleigh number has had to be increased to 1600 to obtain a sustained magnetic field. The initial condition was the same as for Run (A), but at $q = 1$ the initial field seemed to be less critical than at higher values of q . As the critical Rayleigh number for the onset

of convection is not very different from the Run (A) and (B) cases, this means this run is at a much more supercritical Rayleigh number. The behaviour is very chaotic, with the field frequently reversing (Fig. 11). An unattractive feature is that the toroidal field, and to a lesser extent the poloidal field, is very broken up (Fig. 12). The dipole component of the axisymmetric meridional field is small compared with the general field strength, in contrast to the Earth's field where the dipole component dominates. We believe that these solutions are adequately resolved spatially, and increasing the number of modes used did not significantly alter the results, but nevertheless the nature of the solution is such that complete convergence is much less certain for this run than in the other runs described. For this run the time step had to be reduced, otherwise the program crashed, owing to inadequate temporal resolution. The nonaxisymmetric components of the field also have a fairly small-scale structure (Fig. 13). The convection pattern is, however, still reasonably coherent (Fig. 14).

An important question is why the convection has to be so strongly supercritical before dynamo action occurs at $q = 1$ when at $q = 10$ dynamos are obtained at mildly supercritical Ra. A clue

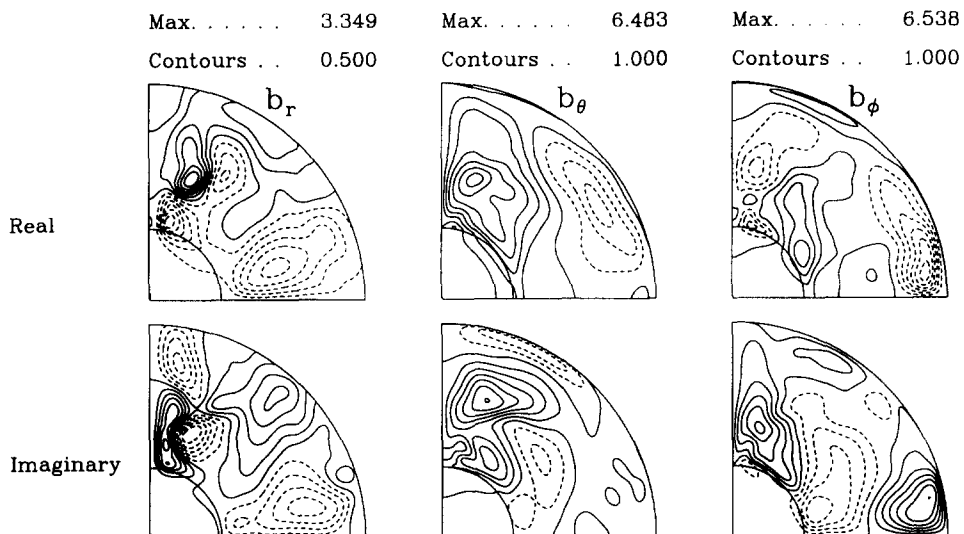


Fig. 8. Nonaxisymmetric magnetic field in Run (B). Negative contours are dashed. The maximum absolute value of each quantity is shown, together with the interval between each contour level.

may be provided by the magnitude of the convective flow (Fig. 14), which is similar to that in the previous runs despite the much larger Ra; in (5) T' is $O(1)$ when Ra becomes large, so that if the magnetic field is not dominant u will scale with qRa rather than Ra alone.

4.4. Run (D)

In Run (D) the initial temperature profile is taken as $r^3/3 - r^2/2$, which is unstable for $\frac{1}{2} < r < 1$ but stable for $1 < r < \frac{3}{2}$, i.e. stable in the outer half of the outer core. Fixed flux boundary

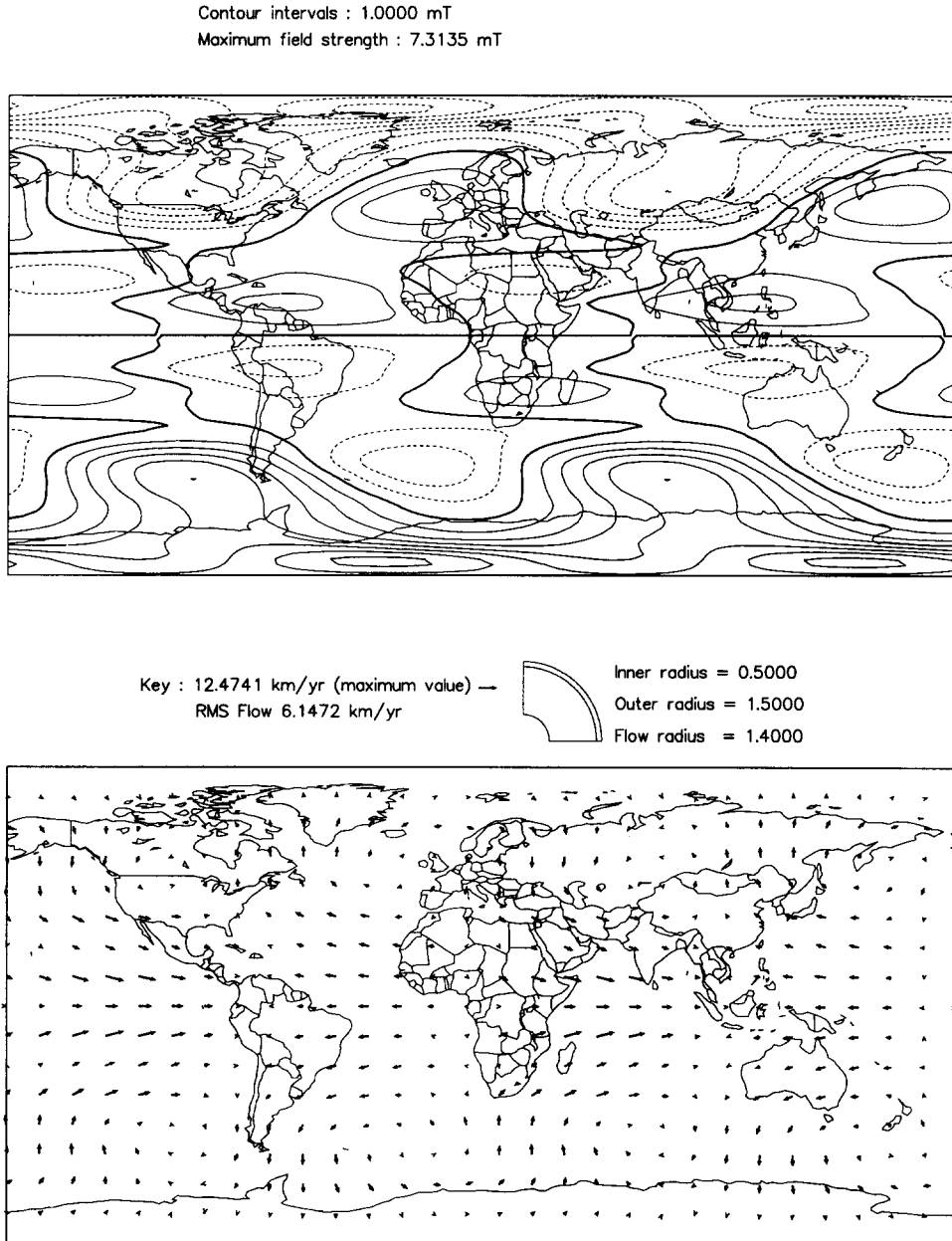


Fig. 9. Run (B). Upper part: the radial component of magnetic field at the CMB. Negative contours are dashed. Lower part: the fluid flow at a radius of 1.4 in dimensionless units.

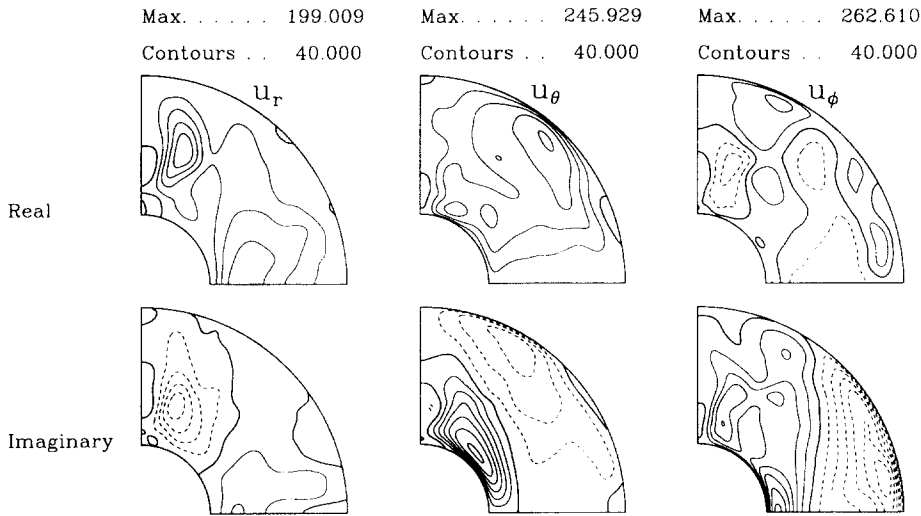


Fig. 10. Nonaxisymmetric velocity field in Run (B). Negative contours are dashed. The maximum absolute value of each quantity is shown, together with the interval between each contour level. The contours give local magnetic Reynolds number.

conditions have been taken for the temperature at the ICB and CMB. The motivation is to see whether this can correct the problem of the excessive nonaxisymmetric field at the CMB. The

justification would be that impurity-enriched material has accumulated over the ages in the top half of the outer core to form a stably stratified zone (e.g. Gubbins et al., 1982). No detailed compositional convection model is proposed.

The parameters for this run are $q = 10$, $E = 5 \times 10^{-4}$ and $Ra = 1300$. This value of Ra may seem large but is not really, because the effective thickness of the unstable layer has been reduced and the gradient of the new profile is less steep. The initial condition was the same as for Run (B). The solution shown (Fig. 15) is definitely of the strong field branch type, i.e. broadly similar to Run (B). Although the solution is still chaotic, and the fluctuations in azimuthal and meridional velocity are still large, the fluctuations in the axisymmetric field are much smaller. The meridional and toroidal field patterns (Fig. 16) also do not vary as much as in the fully unstably stratified layer. This solution does indeed solve the problem of excessive nonaxisymmetric fields near the CMB (Figs. 17 and 18). The radial component of the flow is reduced near the CMB (Fig. 19), and so, although the toroidal field is strong, the non-axisymmetric field produced by advection of the main toroidal field is less. Indeed, the nonaxisymmetric field components are now too small! The

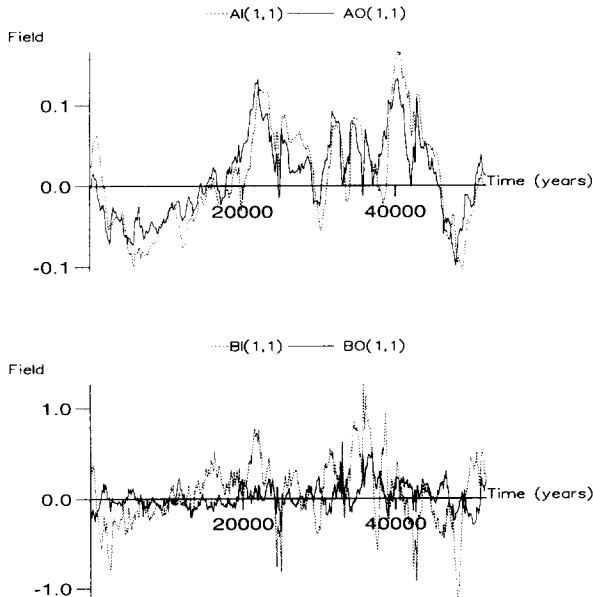


Fig. 11. The time dependence of $AI(1, 1) = A_{11}^{(1)}$, $AO(1, 1) = A_{11}^{(0)}$, $BI(1, 1) = B_{11}^{(1)}$, $BO(1, 1) = B_{11}^{(0)}$ for Run (C).

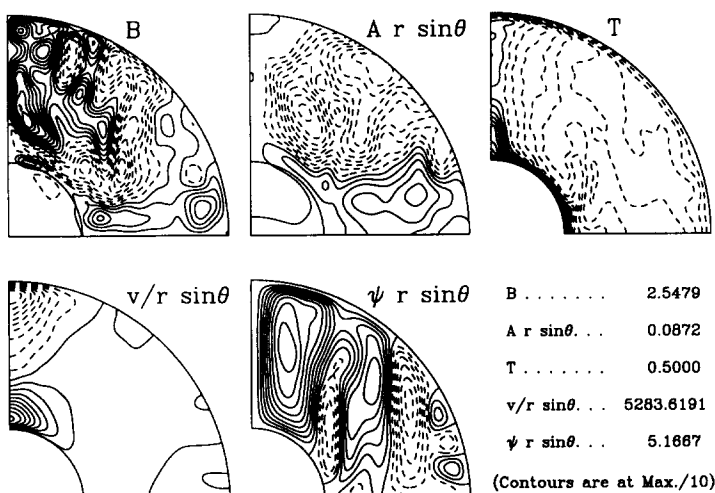


Fig. 12. Axisymmetric variables in Run (C). B , Toroidal field contours; $A r \sin \theta$, meridional field lines; T , temperature contours; $v/r \sin \theta$, angular velocity contours; $\psi r \sin \theta$, meridional stream lines. Negative contours are dashed.

flow at the CMB is also somewhat lower now than that given by Bloxham and Jackson (1991).

The reason for choosing a relatively thick, mildly subadiabatic stable zone was to avoid numerical problems. However, we have done runs with a thinner but more strongly subadiabatic layer, and we found similar reduction of the nonaxisymmetric field components at the CMB.

5. Energy balance

A major difficulty with the geodynamo problem is that the numerical codes used are inevitably lengthy, and so the question of how possible errors in the code can be detected is of great importance. Our code has been built out of the magnetoconvection code and the $\alpha\omega$ axisym-

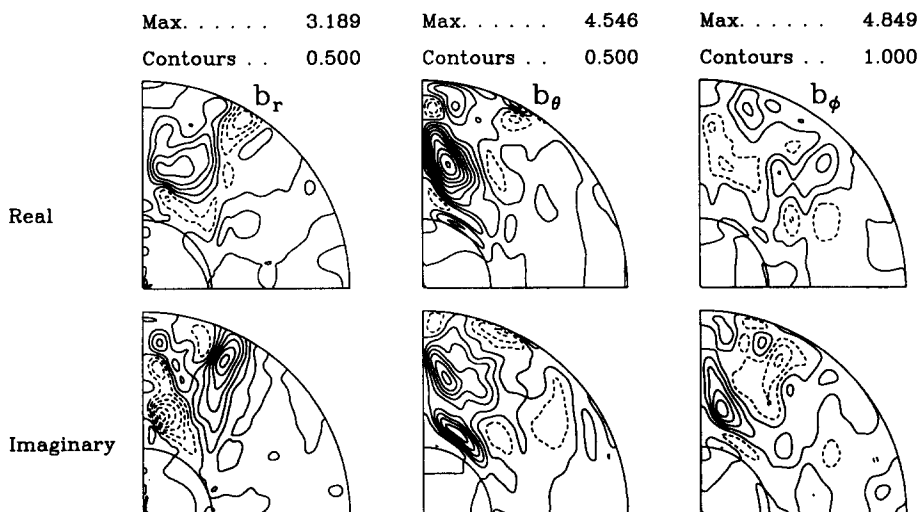


Fig. 13. Nonaxisymmetric magnetic field in Run (C). Negative contours are dashed. The maximum absolute value of each quantity is shown, together with the interval between each contour level.

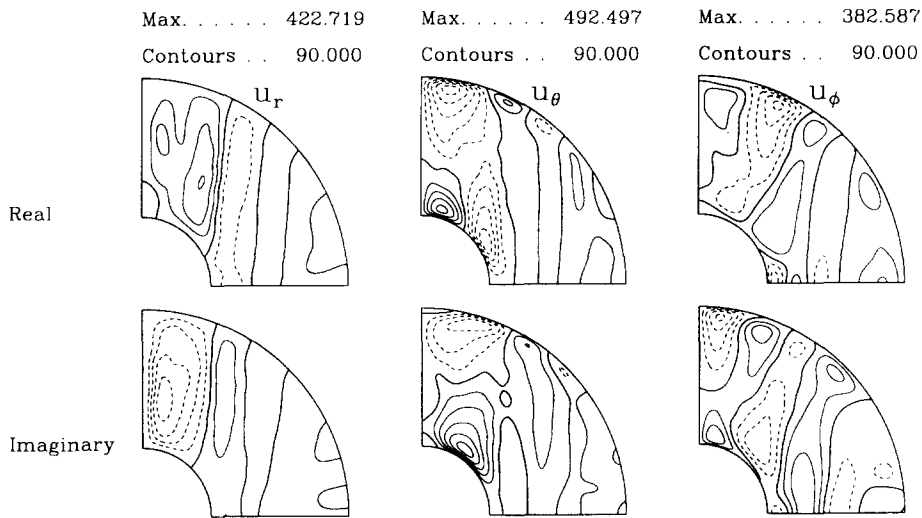


Fig. 14. Nonaxisymmetric velocity field in Run (C). Negative contours are dashed. The maximum absolute value of each quantity is shown, together with the interval between each contour level. The contours give local magnetic Reynolds number.

metric code, both of which have been subjected to rigorous comparisons against codes written by others (Keke Zhang and Gary Glatzmaier). The

only check of the whole code is, however, internal self-consistency; we therefore formed the energy integrals and evaluated the various terms to see if there was overall balance.

For the nonaxisymmetric terms we take the scalar product of (5) with \mathbf{u} and integrate over the outer core. The Coriolis term makes no contribution, and the pressure term vanishes by using the divergence theorem and the fact that the radial velocity vanishes on the boundaries, so we obtain

$$\int_{V_o} \mathbf{u} \cdot [(\nabla \times \bar{\mathbf{B}}) \times \mathbf{b} + (\nabla \times \mathbf{b}) \times \bar{\mathbf{B}}] dV + E \int_{V_o} \mathbf{u} \nabla^2 \mathbf{u} dV + qRa \int_{V_o} \mathbf{u} \cdot \mathbf{r} T' dV = 0 \quad (21)$$

We now multiply the nonaxisymmetric induction equation (6) by \mathbf{b} and integrate over the outer core, and do the same integral over the inner core and add. After further use of the

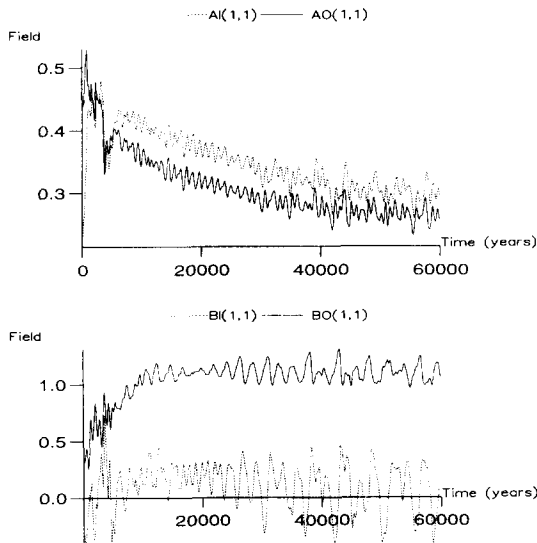


Fig. 15. The time dependence of $AI(1, 1) = A_{11}^{(o)}$, $AO(1, 1) = A_{11}^{(i)}$, $BI(1, 1) = B_{11}^{(o)}$, $BO(1, 1) = B_{11}^{(i)}$ for Run (D).

divergence theorem and boundary conditions, we obtain

$$\begin{aligned} & \int_{V_i+V_o+V_\infty} \frac{\partial |\mathbf{b}|^2}{\partial t} \frac{dV}{2} \\ &= - \int_{V_i+V_o} (\nabla \times \mathbf{b}) \cdot (\nabla \times \mathbf{b}) dV \\ &\quad - \Omega_i r_i^3 \int_0^\pi \int_0^{2\pi} (b_r b_\phi) |_{r=r_i} \sin^2 \theta d\theta d\phi \\ &- \int_{V_o} \bar{\mathbf{U}} \cdot (\nabla \times \mathbf{b}) \times \mathbf{b} + \mathbf{u} \cdot (\nabla \times \mathbf{b}) \times \bar{\mathbf{B}} dV \quad (22) \end{aligned}$$

where V_∞ is the volume of all space outside the outer core. As the magnetic energy outside the core (the observed field) changes, it appears in the overall energy balance. This term can be evaluated as a surface integral at the CMB,

$$\begin{aligned} & \int_{V_\infty} \frac{\partial |\mathbf{b}|^2}{\partial t} \frac{dV}{2} \\ &= \int_S (\mathbf{j} \times \mathbf{b}) \cdot d\mathbf{S} \\ &= -r_o^2 \int_0^\pi \int_0^{2\pi} (b_\theta j_\phi) |_{r=r_o} \sin \theta d\theta d\phi \quad (23) \end{aligned}$$

As the current is continuous at the ICB (conductivity in the inner and outer core being the same)

there is no equivalent term there. The surface term at $r = r_i$ represents the rate of working of electromagnetic stresses from the nonaxisymmetric field on the inner core. As the mantle is insulating in our model, there is no such term at the CMB.

We now do exactly the same for the axisymmetric equations, multiplying them by the corresponding axisymmetric variables and integrating. The surface terms at the ICB and CMB are also treated similarly. Adding (21) plus (22) and the corresponding axisymmetric equations together we obtain the energy equation

$$\frac{\partial \mathcal{M}}{\partial t} = \mathcal{F} + \mathcal{V} + \mathcal{B} \quad (24)$$

where

$$\begin{aligned} \mathcal{M} &= \int_{V_i+V_o+V_\infty} \frac{|\bar{\mathbf{B}}|^2}{2} + \frac{|\mathbf{b}|^2}{2} dV \\ \mathcal{F} &= - \int_{V_i+V_o} (\nabla \times \bar{\mathbf{B}}) \cdot (\nabla \times \bar{\mathbf{B}}) \\ &\quad + (\nabla \times \mathbf{b}) \cdot (\nabla \times \mathbf{b}) dV \\ &\quad - \Omega_i r_i^3 \int_0^\pi \int_0^{2\pi} (b_r b_\phi + \bar{B}_r \bar{B}_\phi) |_{r=r_i} \sin^2 \theta d\theta d\phi \end{aligned}$$

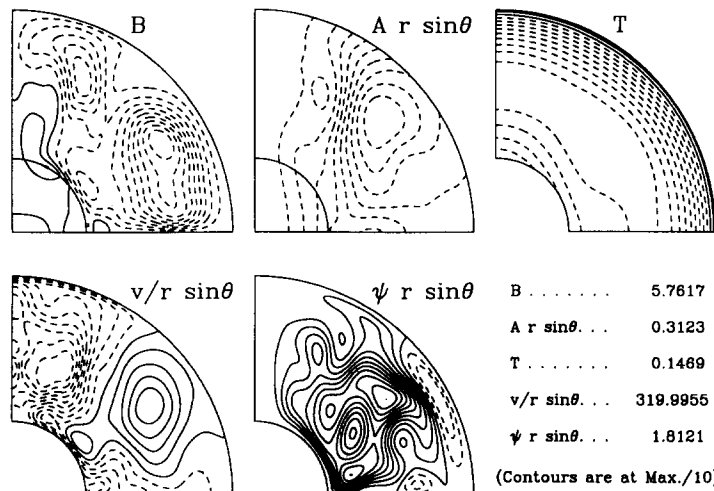


Fig. 16. Axisymmetric variables in Run (D). B , Toroidal field contours; $A r \sin \theta$, meridional field lines; T , temperature contours; $v/r \sin \theta$, angular velocity contours; $\psi r \sin \theta$, meridional stream lines. Negative contours are dashed.

$$\mathcal{V} = E \int_{V_o} \bar{\mathbf{U}} \cdot \nabla^2 \bar{\mathbf{U}} \, dV + E \int_{V_o} \mathbf{u} \cdot \nabla^2 \mathbf{u} \, dV$$

$$\mathcal{B} = q\text{Ra} \int_{V_o} \mathbf{u} \cdot \mathbf{r} T' \, dV + q\text{Ra} \int_{V_o} \bar{\mathbf{U}} \cdot \mathbf{r} \bar{T} \, dV$$

Here \mathcal{M} is the energy in the magnetic field, \mathcal{J} is the Joule dissipation in the inner and outer core, together with the term coming from the magnetic torque on the inner core. This latter term can be rewritten in terms of the rate of working of the viscous torque on the inner core using (11). \mathcal{V} is the rate of viscous dissipation in the outer core (the sum of the viscous and Joule dissipation can be shown to be negative definite by transforming to integrals involving the square of the vorticity together with a negative definite surface term and using (11); see Hollerbach and Jones (1993a) for details). The term \mathcal{B} is the rate of working of the buoyancy forces. This can be evaluated from the temperature equation.

We multiply the nonaxisymmetric temperature equation by $q\text{Ra}T'$ and integrate over the outer

core. Again using the divergence theorem and recalling that $\nabla T_0 = -\mathbf{r}$ we obtain

$$\begin{aligned} q\text{Ra} \int_{V_o} \frac{\partial T'^2}{\partial t} \frac{dV}{2} &= q^2\text{Ra} \int_{V_o} T' \nabla^2 T' \, dV + q\text{Ra} \int_{V_o} \mathbf{u} \cdot \mathbf{r} T' \, dV \\ &\quad + q\text{Ra} \int_{V_o} \bar{\mathbf{T}} \mathbf{u} \cdot \nabla T' \, dV \end{aligned} \tag{25}$$

We now do exactly the same for the axisymmetric temperature equation, multiplying by $q\text{Ra}\bar{T}$ and integrating. Adding the equations together we obtain

$$\frac{\partial \mathcal{M}}{\partial t} - \mathcal{J} - \mathcal{V} = \frac{\partial \mathcal{F}}{\partial t} - \mathcal{S} \tag{26}$$

where

$$\mathcal{F} = q\text{Ra} \int_{V_o} \frac{\bar{T}^2}{2} \, dV + q\text{Ra} \int_{V_o} \frac{T'^2}{2} \, dV$$

$$\mathcal{S} = q^2\text{Ra} \int_{V_o} \bar{T} \nabla^2 \bar{T} \, dV + q^2\text{Ra} \int_{V_o} T' \nabla^2 T' \, dV$$

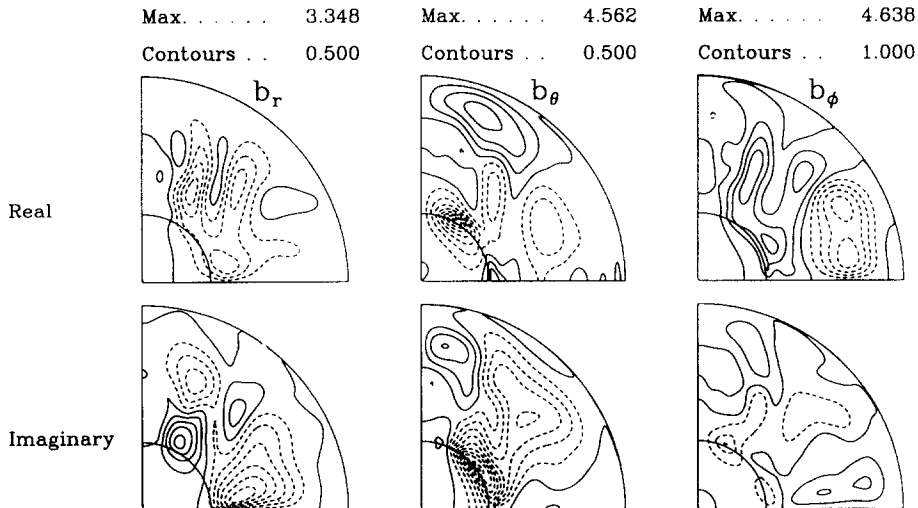


Fig. 17. Nonaxisymmetric magnetic field in Run (D). Negative contours are dashed. The maximum absolute value of each quantity is shown, together with the interval between each contour level.

The individual terms calculated at one time are listed in Table 1 for Runs (A) and (B). Clearly, the exact values depend on the particular time chosen, but the table shows how well the overall energy balance sums to zero. It is also noticeable that although the inner core has an important

role in the dynamics, it is not important in the overall energy balance. It is also of note that in the strong field solutions although the ohmic dissipation is larger than the viscous dissipation in the axisymmetric components, the reverse is true for the nonaxisymmetric components.

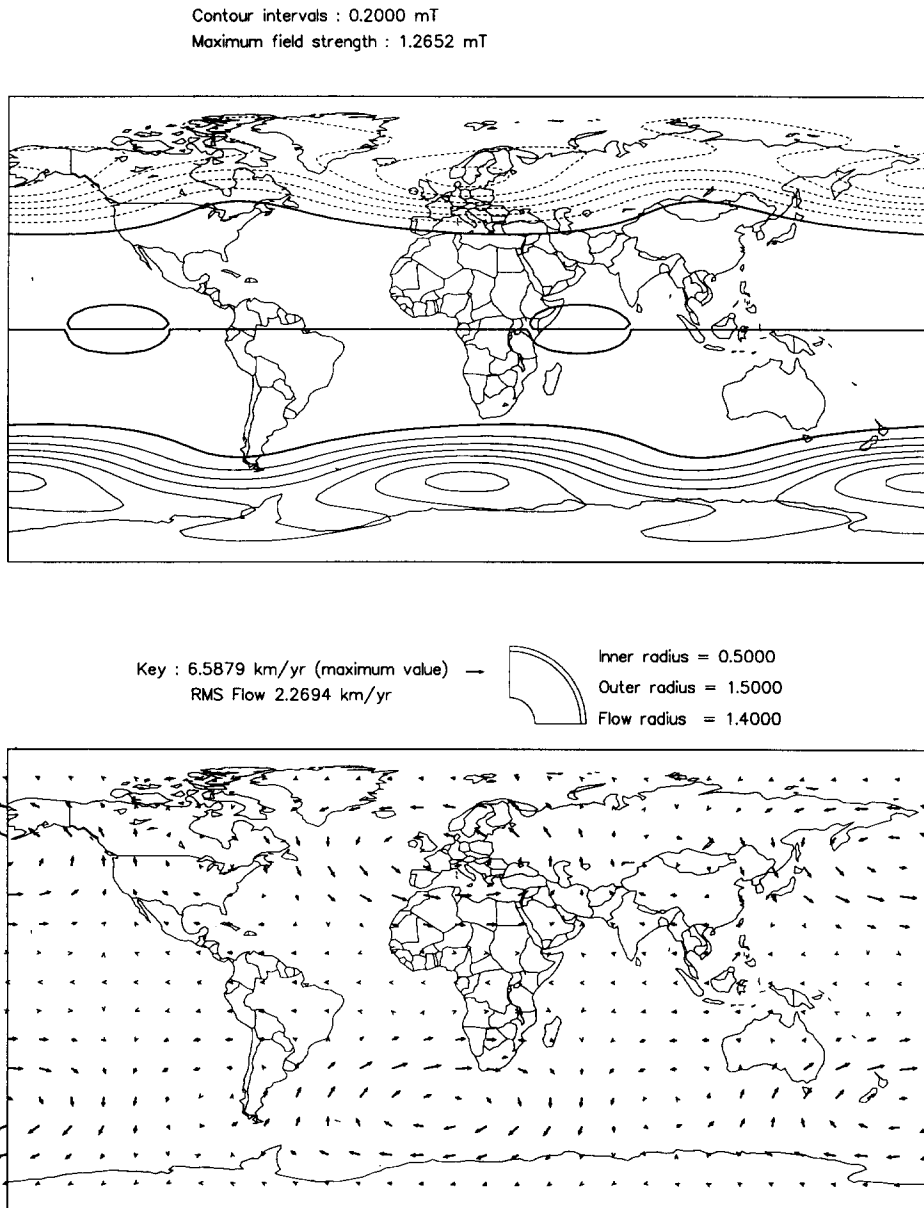


Fig. 18. Run (D). Upper part: the radial component of magnetic field at the CMB. Negative contours are dashed. Lower part: the fluid flow at a radius of 1.4 in dimensionless units.

6. Discussion

These preliminary results are very encouraging. Before the program was run, it was by no means certain that any magnetic field would be generated, let alone one that resembles the Earth's field. It is now clear that not only are fields generated, but they are also of the right order of magnitude and are associated with velocity fields consistent with those deduced from the secular variation and length of day calculations. This must surely make the basic model of the Earth as a convection-driven dynamo a great deal more plausible.

It should, however, be remembered that in our mean field approach the $m = 2$ mode has been imposed, rather than naturally emerging from the calculations. The results of the linear magnetoconvection study L_{JH}95 suggest that $m = 2$ is a preferred mode in a significant area of the parameter space, but it is still an open question as to whether $m = 2$ would necessarily dominate in a fully three-dimensional simulation. This is an important point, because to a large extent it is the dominance of the $m = 2$ mode in the observations that makes the similarity between our calculations and the geomagnetic field as close as it is. Also, we have imposed dipole symmetry about

the equator, and the dipole component dominates over the quadrupole component of the observed geomagnetic field. It is possible that if quadrupole modes had been allowed in our calculation, the agreement with observation would have been less good. The choice of dipole modes only is not inherent in the mean field approximation, and work is in progress on models in which both quadrupole and dipole modes are present.

Of course, much remains to be done. The model must be tested by independently written codes, and exploration of the parameter space has hardly started. We also need comparisons with fully three-dimensional codes to check that our approximations are giving qualitatively reliable results. However, it is clear where some of the fundamental difficulties lie. The two parameters E and q both have very small molecular values in the outer core, and it will be difficult to attain these. Although more attention has been paid to the smallness of E , it may turn out that it is the small value of q which will give the most difficulty. Indeed, at very low q it is impossible to have only large-scale convection if there is a significant shear, as the critical Rayleigh number becomes very large if R_m is much greater than q . There must be turbulent mixing in the core if the flow is convectively driven. What then is the form

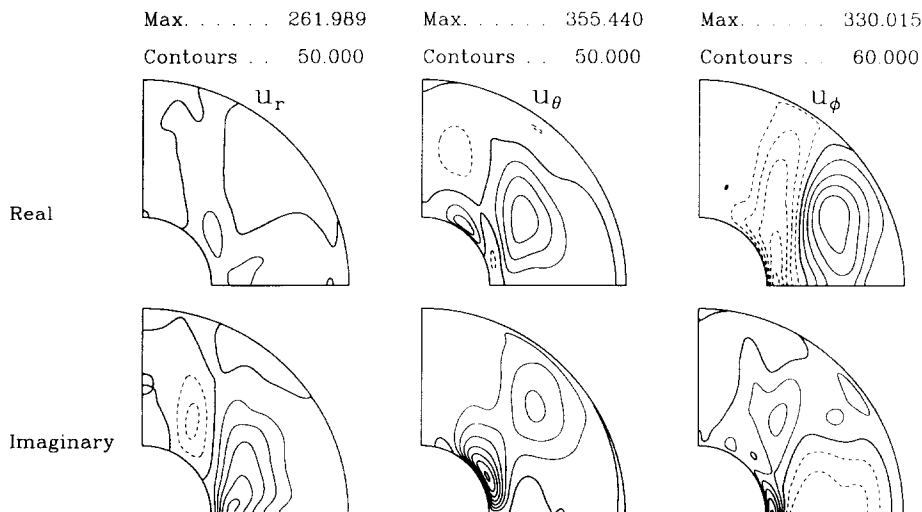


Fig. 19. Nonaxisymmetric velocity field in Run (D). Negative contours are dashed. The maximum absolute value of each quantity is shown, together with the interval between each contour level. The contours give local magnetic Reynolds number.

of convection at low q ? The most likely scenario is that convection at low q is unstable and breaks down very quickly into smaller length scales. These then transport heat (or compositional differences) as turbulent diffusion and so allow large-scale motion to occur. Modelling this process numerically is likely to be very hard, and so we may well be restricted to moderate q and have to assume there is turbulent thermal diffusion which acts in a manner equivalent to an enhanced molecular diffusion process. The way in

which the diffusive processes are modelled is likely to become a vital issue in geodynamo theory. Given our present ignorance about turbulent diffusivity, this issue may only be resolved by comparison between models and observations, rather than from theoretical considerations alone.

A further difficulty is the uncertainty over the driving mechanism and the nature of the appropriate boundary conditions for compositional convection. If it turns out that the Coriolis and Lorentz forces determine the pattern of convec-

Table 1
Energy balance

Energy	Run (A)	Run (B)
Axisymmetric		
$- \int_{V_i} (\nabla \times \bar{\mathbf{b}}_i) \cdot (\nabla \times \bar{\mathbf{b}}_i) dV$	-0.02	-13.31
$- \int_{V_o} (\nabla \times \bar{\mathbf{b}}_o) \cdot (\nabla \times \bar{\mathbf{b}}_o) dV$	-44.22	-1193.81
$E \int_{V_o} \bar{\mathbf{u}} \nabla^2 \bar{\mathbf{u}} dV$	-828.93	-301.65
$-\Omega_i r_i^3 \int_0^\pi \int_0^{2\pi} \bar{\mathbf{b}}_r \cdot \bar{\mathbf{b}}_\phi _{r=r_i} \sin^2 \theta d\theta d\phi$	-0.01	2.56
$-q^2 \text{Ra} \int_{V_o} \bar{T} \nabla^2 \bar{T} dV$	8282.89	2773.14
$- \int_{V_i} \frac{\partial \bar{\mathbf{b}}_i ^2}{\partial t} dV$	0.00	16.02
$- \int_{V_o} \frac{\partial \bar{\mathbf{b}}_o ^2}{\partial t} dV$	-2.69	5.17
$- \int_{V_\infty} \frac{\partial \bar{\mathbf{b}}_o ^2}{\partial t} dV$	-0.02	-16.80
$q \text{Ra} \int_{V_o} \frac{\partial \bar{T}^2}{\partial t} dV$	8.73	-182.67
Axisymmetric energy	7415.73	1088.65
Non-axisymmetric		
$- \int_{V_i} (\nabla \times \mathbf{b}_i) \cdot (\nabla \times \mathbf{b}_i) dV$	-0.01	-1.50
$- \int_{V_o} (\nabla \times \mathbf{b}_o) \cdot (\nabla \times \mathbf{b}_o) dV$	-45.25	-1747.15
$E \int_{V_o} \mathbf{u} \nabla^2 \mathbf{u} dV$	-14826.91	-2737.87
$-\Omega_i r_i^3 \int_0^\pi \int_0^{2\pi} b_r \cdot b_\phi _{r=r_i} \sin^2 \theta d\theta d\phi$	0.00	-2.82
$-q^2 \text{Ra} \int_{V_o} T' \nabla^2 T' dV$	7430.14	3384.60
$- \int_{V_i} \frac{\partial \mathbf{b}_i ^2}{\partial t} dV$	0.01	-1.07
$- \int_{V_o} \frac{\partial \mathbf{b}_o ^2}{\partial t} dV$	-7.01	192.68
$- \int_{V_\infty} \frac{\partial \mathbf{b}_o ^2}{\partial t} dV$	1.59	41.19
$q \text{Ra} \int_{V_o} \frac{\partial T'^2}{\partial t} dV$	31.68	-216.66
Non-axisymmetric energy	-7415.76	-1088.60
Total energy	-0.03	0.05

tion it may be that the different models produce results that are not too dissimilar. This is good for dynamo modelling, but the corollary is that even when the dynamo process is understood, it may be difficult to discriminate between the different possible driving mechanisms.

Finally, the emergence of strong field and weak field dynamos in this model is very helpful. This ties in with experience gained from magnetoconvection and α -effect models. The fact that the strong field models do not reverse (or reverse infrequently) may seem a disadvantage to those unfamiliar with α -effect models, but in fact a major difficulty with models where the toroidal field is significantly stronger than the poloidal field is that they usually reverse too often.

Acknowledgements

This work was funded by the PPARC under Grant GR/E93251.

References

- Abdel-Aziz, M.M. and Jones, C.A., 1988. $\alpha\omega$ -dynamos and Taylor's constraint. *Geophys. Astrophys. Fluid Dyn.*, 44: 117–139.
- Anufriev, A.P., Cupal, I. and Hejda, P., 1995. Taylor state in $\alpha\omega$ -dynamo. *Geophys. Astrophys. Fluid Dyn.*, in press.
- Barenghi, C.F., 1992. Nonlinear planetary dynamos in a rotating spherical shell II, The post Taylor equilibration for α^2 -dynamos. *Geophys. Astrophys. Fluid Dyn.*, 67: 27–36.
- Barenghi, C.F., 1993. Nonlinear planetary dynamos in a rotating spherical shell III, $\alpha^2\omega$ -models and the geodynamo. *Geophys. Astrophys. Fluid Dyn.*, 71: 163–185.
- Barenghi, C.F. and Jones, C.A., 1991. Nonlinear planetary dynamos in a rotating spherical shell. *Geophys. Astrophys. Fluid Dyn.*, 60: 211–243.
- Bloxham, J. and Jackson, A., 1991. Fluid flow near the surface of Earth's outer core. *Rev. Geophys.*, 29: 97–120.
- Bloxham, J., Gubbins, D. and Jackson, A., 1989. Geomagnetic secular variation. *Philos Trans. R. Soc. London, Ser. A*, 329: 415–502.
- Braginsky, S.I., 1976. On the nearly axisymmetric model of the hydrodynamic dynamo of the Earth. *Phys. Earth Planet. Inter.*, 11: 191–199.
- Braginsky, S.I., 1978. An almost axially symmetric model of the hydrodynamic dynamo of the Earth II. *Geomagn. Aeron.*, 18: 340–351.
- Braginsky, S.I. and Roberts, P.H., 1987. A model-Z geodynamo. *Phys. Earth Planet. Inter.*, 38: 327–349.
- Cowling, T.G., 1934. The magnetic field of sunspots. *Mon. Not. R. Astron. Soc.*, 94: 39–48.
- Cuong, P.G. and Busse, F.H., 1981. Generation of magnetic fields by convection in a rotating sphere. I. *Phys. Earth Planet. Inter.*, 24: 272–283.
- Fearn, D.R., 1994. Nonlinear planetary dynamos, In: M.R.E. Proctor and A.D. Gilbert (Editors), *Stellar and Planetary Dynamos*, Cambridge University Press, Cambridge.
- Fearn, D.R. and Proctor, M.R.E., 1984. Self-consistent dynamo models driven by hydrodynamic instabilities. *Phys. Earth Planet. Inter.*, 36: 78–84.
- Fearn, D.R. and Proctor, M.R.E., 1987. On the computation of steady, self-consistent, spherical dynamos. *Geophys. Astrophys. Fluid Dyn.*, 38: 293–325.
- Fearn, D.R., Proctor, M.R.E. and Sellar, C.C., 1994. Nonlinear magnetoconvection in a rapidly rotating sphere and Taylor's constraint. *Geophys. Astrophys. Fluid Dyn.*, 77: 111–132.
- Glatzmaier, G. and Roberts, P.H., 1995. A three-dimensional convective dynamo solution with rotating and finitely conducting inner core and mantle. *Phys. Earth Planet. Inter.*, 91: 63–75.
- Gubbins, D. and Bloxham, J., 1987. Morphology of the geomagnetic field and implications for the geodynamo. *Nature* 325: 509–511.
- Gubbins, D., Thompson, C.J. and Whaler, K.A., 1982. Stable regions in the Earth's liquid core. *Geophys. J. R. Astron. Soc.*, 68: 241–251.
- Hirsching, W. and Busse, F.H., 1995. Stationary and chaotic dynamos in rotating spherical shells. *Phys. Earth Planet. Inter.*, 90: 243–254.
- Hollerbach, R., 1994a. Magneto-hydrodynamic Ekman and Stewartson layers in a rotating spherical shell. *Proc. R. Soc. London, Ser. A*, 444: 333–346.
- Hollerbach, R., 1994b. Imposing a magnetic field across a nonaxisymmetric shear layer in a rotating spherical shell. *Phys. Fluids*, 6: 2540–2544.
- Hollerbach, R. and Lerley, G.R., 1991. A modal α^2 -dynamo in the limit of asymptotically small viscosity. *Geophys. Astrophys. Fluid Dyn.*, 60: 133–158.
- Hollerbach, R. and Jones, C.A., 1993a. A geodynamo model incorporating a finitely conducting inner core. *Phys. Earth Planet. Inter.*, 75: 317–327.
- Hollerbach, R. and Jones, C.A., 1993b. Influence of the Earth's inner core on geomagnetic fluctuations and reversals. *Nature*, 365: 541–543.
- Hollerbach, R. and Jones, C.A., 1995. On the magnetically stabilizing role of the Earth's inner core. *Phys. Earth Planet. Inter.*, 87: 171–181.
- Hollerbach, R., Barenghi, C.F. and Jones, C.A., 1992. Taylor's constraint in a spherical $\alpha\omega$ -dynamo. *Geophys. Astrophys. Fluid Dyn.*, 65: 3–25.
- Hughes, D.W., 1993. Testing for dynamo action, In: M.R.E. Proctor, P.C. Matthews and A.M. Rucklidge (Editors), *Solar and Planetary Dynamos*. Cambridge University Press, Cambridge.

- Jault, D., 1995. Model Z by computation and the Taylor's condition. *Geophys. Astrophys. Fluid Dyn.*, in press.
- Jones, C.A. and Wallace, S.G., 1992. Periodic, chaotic and steady solutions in $\alpha\omega$ -dynamoes. *Geophys. Astrophys. Fluid Dyn.*, 67: 37–64.
- Krause, F. and Rädler, K.H., 1980. *Mean-Field Magnetohydrodynamics and Dynamo Theory*, Pergamon, Oxford.
- Longbottom, A.W., Jones, C.A. and Hollerbach, R., 1995. Linear magnetoconvection in a rotating spherical shell, incorporating a finitely conducting inner core. *Geophys. Astrophys. Fluid Dyn.*, in press.
- Malkus, M.V.R. and Proctor, M.R.E., 1975. The macrodynamics of α -effect dynamoes in rotating fluids. *J. Fluid Mech.*, 67: 417–443.
- Proctor, M.R.E., 1977. Numerical solutions of the non-linear α -effect dynamo equations. *J. Fluid Mech.* 80: 769–784.
- Roberts, P.H., 1989. From Taylor state to model-Z? *Geophys. Astrophys. Fluid Dyn.*, 49: 143–160.
- Soward, A.M. and Jones, C.A., 1983. α^2 -dynamoes and Taylor's constraint. *Geophys. Astrophys. Fluid Dyn.*, 27: 87–122.
- Taylor, J.B., 1963. The magnetohydrodynamics of a rotating fluid and the Earth's dynamo problem. *Proc. R. Soc. London, Ser. A*, 274: 274–283.
- Zhang, K. and Busse, F.H., 1988. Finite amplitude convection and magnetic field generation in a rotating spherical shell. *Geophys. Astrophys. Fluid Dyn.*, 44: 33–54.
- Zhang, K. and Busse, F.H., 1989. Convection driven magnetohydrodynamic dynamoes in rotating spherical shells. *Geophys. Astrophys. Fluid Dyn.*, 49: 97–116.
- Zhang, K. and Busse, F.H., 1990. Generation of magnetic fields by convection in a rotating spherical fluid shell of infinite Prandtl number. *Phys. Earth Planet. Inter.*, 59: 208–222.